



Published in final edited form as:

*Int J Radiat Oncol Biol Phys.* 2019 March 01; 103(3): 719–727. doi:10.1016/j.ijrobp.2018.10.007.

## Interleukin 6 Signaling Blockade Exacerbates Acute and Late Injury From Focal Intestinal Irradiation

Brett I. Bell, MS<sup>\*,†</sup>, Sravya Koduri, BS<sup>\*</sup>, Carlo Salas Salinas<sup>\*</sup>, James Monslow, PhD<sup>‡</sup>, Ellen Puré, PhD<sup>‡</sup>, Edgar Ben-Josef, MD<sup>\*</sup>, Constantinos Koumenis, PhD<sup>\*</sup>, Ioannis I. Verginadis, PhD<sup>\*</sup>

<sup>\*</sup>Department of Radiation Oncology, Perelman School of Medicine, University of Pennsylvania, Philadelphia, Pennsylvania

<sup>†</sup>Department of Chemistry, School of Arts and Sciences, University of Pennsylvania, Philadelphia, Pennsylvania

<sup>‡</sup>Department of Biomedical Sciences, School of Veterinary Medicine, University of Pennsylvania, Philadelphia, Pennsylvania

### Abstract

**Purpose:** To evaluate the acute changes in leukocyte populations after focal irradiation and to assess the role of interleukin 6 (IL-6) in acute and late radiation injury.

**Methods and Materials:** Mice were surgically implanted with a radiopaque marker on the surface of the small intestine. Mice were then imaged with cone beam computed tomography to locate the marker and irradiated with 18 Gy of 5 × 5 mm collimated x-rays onto the marked intestine using the Small Animal Radiation Research Platform. Intestinal sections and blood were harvested 1, 3.5, 7, and 14 days and 2 months post-irradiation (post-IR) for histology and complete blood count, respectively. Immune cell populations were assessed by immunofluorescence in the acute phase. Collagen deposition was assessed 2 months post-IR. IL-6<sup>-/-</sup> intestinal sections were assessed post-IR for morphology, EdU, Ki67, and TUNEL in comparison to IL-6<sup>+/+</sup> mice. Furthermore, a set of IL-6<sup>+/+</sup> mice were treated with anti-IL-6R to assess the role of IL-6 in late intestinal injury.

**Results:** Intestinal radiation damage peaked 14 days post-IR, and fibrosis had developed by 60 days post-IR. There was a marked infiltration of immune cells into the irradiated intestine, with increased neutrophils, macrophages, B-cells, and CD4<sup>+</sup> T cells maintained from 3.5 to 14 days post-IR. CD8<sup>+</sup> T cells were decreased from days 7 to 14 post-IR. Systemically, leukocytes were increased in the peripheral blood 14 days post-IR with anemia being maintained from 14 days to 2 months. IL-6 was significantly increased in the serum post-IR. IL-6<sup>-/-</sup> mice demonstrated worsened intestinal injury acutely post-IR. Moreover, anti-IL-6R-treated mice presented with worsened intestinal fibrosis 2 months post-IR.

Reprint requests to: Ioannis I. Verginadis, PhD, University of Pennsylvania, Perelman School of Medicine, 3400 Civic Center Blvd., Bldg. 421, Smilow Center for Translational Research, Room 8-160, Philadelphia, PA 19104-5156. Tel: (215) 898-0076; [vioannis@pennmedicine.upenn.edu](mailto:vioannis@pennmedicine.upenn.edu).

Conflict of interest: none.

Supplementary material for this article can be found at <https://doi.org/10.1016/j.ijrobp.2018.10.007>.

**Conclusions:** Focal irradiation of the intestine produced a significant increase in immune cells in the irradiated area and systemic inflammation and anemia. Blockade of IL-6 signaling was found to exacerbate acute intestinal injury and late intestinal injury after focal irradiation.

## Summary

The time-dependent immune response to focal intestinal irradiation has not been investigated. Therefore, we used immunofluorescence to quantify changes in leukocyte populations after focal irradiation. Subsequently, we investigated the role of interleukin-6 signaling using knockout mice and antibody-mediated signaling blockade. We identified time-dependent fluctuations in leukocyte populations in the irradiated intestine and further noted interleukin-6 signaling blockade exacerbates intestinal radiation injury.

---

## Introduction

Radiation therapy (RT) is indicated for approximately half of all cancer patients.<sup>1,2</sup> However, the therapeutic dose of radiation is limited by the deleterious effects of incidental irradiation of the intestine during the treatment of abdominal or pelvic malignancies. Almost all patients undergoing abdominal or pelvic radiation therapy experience gastrointestinal symptoms.<sup>3</sup> Approximately 20% of these patients have their treatment plan altered because of these adverse effects, risking poor local control of the tumor.<sup>4</sup> Despite advances in technology designed to minimize radiation doses to normal tissue, radiation-induced normal tissue toxicity remains one of the most significant challenges in the treatment of patients with cancer with localized disease. The number of patients living in the United States with postirradiation (post-IR) intestinal dysfunction exceeds 1.6 million, outpacing the approximately 1.4 million who have irritable bowel disease.<sup>5</sup>

There is significant interaction between the many resident cell populations of the intestine after irradiation, including intestinal stem cells and epithelial cells, microvascular endothelial cells, enteric neurons, fibroblasts, and immune cells.<sup>5</sup> The intestinal immune system is of particular interest in this context because it is the largest immune compartment in the body.<sup>6</sup> Most studies of intestinal immune cell involvement post-IR stem from models with large radiation fields, such as in whole abdominal or total body irradiation, and have found leukocyte recruitment to the intestine.<sup>7-10</sup> However, the characterization of the immune infiltrates within focally damaged intestine and the elucidation of the role that key inflammatory cytokines play in the extent or resolution of the incidental radiation damaged has not been assessed in detail.

Consequently, our group developed a clinically relevant animal model that involves a single minimally invasive surgery to implant a radiopaque marker on the surface of the small intestine in situ.<sup>11</sup> The mouse receives image guided focal irradiation to the marked intestine using the Small Animal Radiation Research Platform, allowing the focally irradiated tissue to be studied both in the acute and late phases after radiation exposure. Interleukin-6 (IL-6) is a pleiotropic cytokine that has wide-ranging effects on physiological processes.<sup>12</sup> Inhibition of IL-6 signaling has been implicated in the amelioration of fibrosis in the lung<sup>13</sup> and peritoneum.<sup>14</sup> However, in the intestine, IL-6 appears to be necessary for the survival of intestinal epithelial cells.<sup>15,16</sup> Therefore, we set out to clarify the time course of the immune

response after focal irradiation and to understand the role of IL-6 in acute and late radiation injury.

## Methods and Materials

### Animals

Eight- to 16-week-old male and female C57Bl/6J mice and B6.129S2-Il6<sup>tm1Kopf/J</sup> (The Jackson Laboratory) were maintained in the University of Pennsylvania animal facilities. All experimental procedures were conducted in accordance with protocols approved by the Institutional Animal Care and Use Committee. Eight-week-old mice underwent surgical implantation of a radiopaque marker, recovered for 1 week, and were then subjected to either a computed tomography (CT) scan or a CT scan and 18 Gy of focal irradiation. Mice were euthanized by CO<sub>2</sub> asphyxiation. IL-6 blockade was completed with a 2-mg loading dose intraperitoneally 10 days post-IR and 0.5-mg (Clone 15A7; BioXCell) doses weekly until euthanasia. An isotype control (Clone LTF-2; BioXCell) was also administered.

### Surgery and irradiation

The radiopaque marker made of bismuth subcarbonate was prepared and implanted as described previously.<sup>11</sup> Cone beam CT and irradiation were performed as previously described.<sup>11</sup> A single dose of 18 Gy was delivered focally using a 5 × 5-mm collimated beam. Details are in the Supplemental Methods (available online at <https://doi.org/10.1016/j.ijrobp.2018.10.007>).

### Histology

Intestinal segments measuring 1.5 cm were harvested at the site of marker implantation, as was a site out of the x-ray beam track, for histologic evaluation. Tissues for quantifying leukocyte infiltration were embedded longitudinally in Optimal Cutting Temperature medium and cryosectioned at 5 μm. Tissues for Masson's trichrome and picrosirius red staining were fixed in 10% neutral buffered formalin for 24 hours before dehydration and paraffin embedding. Coded hematoxylin and eosin-stained slides were evaluated by an independent pathologist. Radiation injury scoring was completed as previously described with minor modification.<sup>17</sup>

### Quantitative histology

Immunofluorescent staining for myeloperoxidase (neutrophils), F4/80 (macrophages), CD4 (T-helper lymphocytes), CD8 (cytotoxic T lymphocytes), and CD45R (B lymphocytes) was performed using standard procedures. Leukocyte infiltration was quantified by counting the average number of positive cells in 10 fields within the irradiated area with a 40× objective and 10× ocular.

### EdU, Ki67, and TUNEL assays

Twenty milligrams per kilogram EdU was injected intraperitoneally 2 hours before euthanasia. EdU was detected according to the manufacturer's instructions (Thermo Fisher). Ki67 was assessed on formalin-fixed intestinal samples (Thermo Fisher). TUNEL<sup>+</sup> apoptotic

cells were detected according to manufacturer's instructions (Sigma Aldrich). EdU<sup>+</sup>, Ki67<sup>+</sup>, and TUNEL<sup>+</sup> cells/crypt were assessed by counting 50 intact crypts in the marked region.

### Complete blood count

Mice were euthanized, and blood was immediately collected by cardiac puncture into tubes containing K<sub>2</sub> EDTA. Automated assessment of the blood was conducted using an Idexx Procyte Hematology Analyzer (Idexx Laboratories). White blood cell differential was performed on a blood smear stained with Wright-Giemsa.

### Cytokine microbead assay

A 9-plex cytokine microbead assay was performed on serum at 3.5 and 14 days post-IR as described previously.<sup>11</sup>

### Statistical analysis

Statistical analysis was conducted using GraphPad Prism V software. Survival analysis was conducted using Kaplan-Meier statistics with a log-rank test. For survival studies IL-6<sup>+/+</sup> (n = 8), IL-6<sup>-/-</sup> (n = 3), isotype (n = 6), and anti-IL-6R (n = 6), with an endpoint of 20% weight loss or moribund, were used. For time-course analysis, 1-way ordinary analysis of variance with Dunnett's test was conducted. For EdU, Ki67, and TUNEL analysis, a 2-way analysis of variance with Tukey's multiple comparisons testing was performed. F statistics are presented as (degrees of freedom numerator, and denominator). For single comparisons, an unpaired 2-tailed Student's *t* test was used. The alpha value was set at 0.05. Data presented as mean + standard error of the mean, *n* = 3/group in all experiments.

## Results

### Focal irradiation induces intestinal ulceration

Cone beam CT was used to locate the marker 7 days postsurgery (Fig. 1A), which was followed by image guided irradiation (Fig. 1B). A dose of 18 Gy was well tolerated in the acute phase with minor weight loss and no acute lethality (Fig. 1C). Twenty-two percent of the mice used in this study were euthanized postsurgery but before radiation because of bowel obstruction.

Damage was limited to the marked region of the intestine, with deep mucosal/crypt necrosis and an early accumulation of leukocytes 1 day post-IR (Fig. 1E). Extensive mucosal and crypt necrosis was evident by 3.5 days post-IR with subacute inflammation. Crypt structure was largely ablated by 3.5 days post-IR with subsequent loss of normal villous architecture. Seven to 14 days post-IR, mice exhibited extensive ulceration with re-epithelialization. Early prefibrotic tissue was present 14 days post-IR. A modified version of a published radiation injury scoring system<sup>17</sup> was used to quantify morphologic changes associated with focal irradiation of the small intestine. This demonstrated a time-dependent increase in intestinal radiation injury that peaked at 2 weeks post-IR in the acute phase (Fig. 1D).

### Immune cells are recruited to the irradiated area

Focal irradiation of the marked intestine induced a time-dependent increase in infiltration of myeloperoxidase-positive cells (Fig. 2A, 2B; and Fig. EA1, available online at <https://doi.org/10.1016/j.ijrobp.2018.10.007>), the primary population of which is neutrophils, compared with sham-irradiated intestine. There was initially a slight increase in neutrophil infiltration 1 day post-IR followed by an approximately 7-fold increase in infiltration that persisted from 3.5 to 14 days post-IR. Macrophages also exhibited 2-fold increased infiltration from 3.5 days post-IR persisting to 14 days (Fig. 2C, D).

Although CD4<sup>+</sup> T cells exhibited a marked increase in infiltration at 3.5 to 14 days (Fig. 2E, F), CD8<sup>+</sup> T cells exhibited significantly lower levels from days 7 to 14 post-IR (Fig. 2G, H). CD8<sup>+</sup> lymphocytes normally localized almost entirely to the villi. However, irradiated mice exhibited severe structural changes that altered normal villous morphology, potentially affecting proper localization of CD8<sup>+</sup> T cells. The ablation of villous structure was initially limited to the center of the radiation wound and expanded outward from 3.5 to 14 days. Finally, CD45R<sup>+</sup> B cells demonstrated a 2-fold increase within the irradiated intestine from 3.5 to 7 days post-IR that began to wane by day 14 (Fig. 2I, J). Each leukocyte population exhibited remarkable localization to the irradiated mucosa compared with surrounding unirradiated tissue (Fig. EA2).

### Focal irradiation induces a systemic inflammatory reaction and anemia

Intriguingly, focal irradiation of the intestine using our model induced a systemic inflammatory reaction. There was a significant increase in the number of circulating white blood cells 2 weeks post-IR, driven by increased neutrophils and monocytes (Fig. 3A–C). Additionally, mice exhibited a regenerative anemia characterized by decreased erythrocytes, hemoglobin, and hematocrit (Figs. 3D, 3E; Fig. EA3, available online at <https://doi.org/10.1016/j.ijrobp.2018.10.007>) and increased reticulocytes (Fig. 3F) from 2 weeks to 2 months post-IR that was found by occult blood testing to be the result of gastrointestinal bleeding. The lung is a vulnerable target organ in cases of inflammation.<sup>18</sup> We therefore assessed the lungs after intestinal irradiation and found increased circulating neutrophils present 2 weeks post-IR in blood vessels within the lung, consistent with the findings in the peripheral blood. There was also evidence of neutrophil margination along the endothelial lining of the vascular network, which suggests systemic neutrophil activation (Fig. 3G). Splenic extramedullary hematopoiesis was noted (Fig. 3H) with associated splenomegaly (Fig. EA4), which is further indicative of the hematopoietic stress induced by irradiation.

The serum cytokine profile can serve as a surrogate marker of systemic activation of the immune system. To assess the inflammatory response post-IR, a cytokine microbead assay was performed on serum taken from mice 3.5 and 14 days post-IR. This revealed increases in GM-CSF, IL12p40, IL13, IL17, and tumor necrosis factor- $\alpha$  by 14 days post-IR (Fig. 3I). Furthermore, IL12p70 was undetectable in controls but was detected 14 days post-IR. The most notable change in protein expression was seen with IL-6, which was increased 30-fold. At 3.5 days post-IR the increase in IL-6 was comparable to levels previously observed after 18 Gy.<sup>11</sup> However, the increase in IL-6 levels observed at 14 days post-IR is substantially greater and indicative of an acute phase response.

### IL-6<sup>-/-</sup> mice are sensitive to intestinal irradiation

Previous results in our laboratory showed IL-6 to be involved in the response to intestinal radiation injury.<sup>11</sup> The clear systemic impact of IL-6 in the present study further demonstrated the need to investigate the role of IL-6 in intestinal radiation injury. We found that IL-6 null mice (IL-6<sup>-/-</sup>), syngeneic to C57Bl/6 mice, were sensitized to 18 Gy with a significant decrease in survival post-IR (Fig. 4A) compared with IL-6<sup>+/+</sup> mice. The IL-6<sup>-/-</sup> mice experienced exacerbated early intestinal injury as evidenced by increased crypt necrosis at 1 day post-IR and marked inflammation 3.5 days post-IR. Seven days post-IR, extensive ulceration was noted with edema and crypt loss (Fig. 4B).

Irradiated IL-6<sup>-/-</sup> mice had increased apoptosis within crypts at 1 day post-IR as marked by TUNEL (Fig. 4C, 4D). This is consistent with past results that suggest IL-6 produced by lamina propria myeloid cells protects normal intestinal epithelial cells from apoptosis.<sup>16</sup>

Cell proliferation was assessed by performing crypt microcolony assays in mice using EdU and Ki67 as markers of proliferation. IL-6<sup>+/+</sup> and IL-6<sup>-/-</sup> mice exhibited significant decreases in EdU<sup>+</sup> cells/crypt post-IR, indicating fewer cells in the S-phase of the cell cycle. At this dose of irradiation, IL-6<sup>+/+</sup> and IL-6<sup>-/-</sup> mice showed comparably decreased levels of S-phase cells post-IR (Fig. 4E). We further assessed Ki67<sup>+</sup> cells/crypt, which marked cycling cells. This confirmed the baseline increase in cell proliferation observed in IL-6<sup>-/-</sup> mice with EdU (Fig. 4F, 4G). The higher proliferation at baseline is very likely reactive to the loss of intestinal epithelial cells at baseline. Additionally, the trend toward increased proliferation post-IR is likely similarly reactive toward the significantly increased apoptosis observed in IL-6<sup>-/-</sup> mice. However, the ulceration evident at 7 days post-IR indicates that this reactive proliferation is not able to overcome the reduced intestinal epithelial cell survival. Interestingly, an increase in proliferation was observed at the edge of the irradiation wound, likely to re-epithelialize the barrier among both genotypes (Fig. EA5).

### IL-6 signaling blockade exacerbates intestinal radiation-induced fibrosis

The results with the IL-6<sup>-/-</sup> mice suggested that IL-6 played a role in promoting epithelial cell survival during or shortly after radiation. However, genetic deletion of IL-6 could result in other systemic problems, confounding our results.<sup>12</sup> To address the potential role of IL-6 in intestinal injury using a more physiologically relevant approach, we used antibody-mediated blockade of IL-6 signaling using a previously validated dosing scheme.<sup>19</sup> We optimized our dosing to prevent mortality in the acute phase post-IR by beginning to treat mice with anti-IL-6R on day 10 post-IR. Anti-IL-6R treated mice did not differ from isotype controls in terms of survival or weight post-IR (Fig. 5A, 5B).

Consequential late effects of radiation damage to the small intestine include narrowing of the lumen as a result of collagen deposition and extracellular matrix remodeling. We identified on gross examination that irradiated animals generally exhibited intestinal strictures at the site of marker implantation, which resulted in incomplete bowel obstruction. On histologic examination, both 18 Gy + isotype and 18 Gy + anti-IL-6R-treated groups exhibited signs of intestinal radiation injury compared with the 0 Gy control group. Both irradiated groups showed epithelial atypia with evidence of vascular sclerosis and lymph congestion. The anti-

IL-6R–treated group exhibited significant ulceration and erosion of the epithelium, which was not observed in any of the isotype controls. Irradiated mice further exhibited mural to transmural fibrosis with increased collagen deposition identified by Masson’s trichrome stain (Fig. 5D). The collagen deposition was worsened in the anti-IL-6R–treated group, with additional collagen observed between crypts and submucosally. This finding was confirmed with picrosirius red staining to demonstrate fibrillar collagen.<sup>20</sup> Picrosirius staining demonstrated a significant increase in fibrillar collagen in the anti-IL-6R–treated group compared with the isotype group (Fig. 5C, 5D).

## Discussion

Although the effects of radiation exposure on relatively large volumes of intestine have been studied, little is known about the impact of clinically relevant focal irradiation on the small intestine. Our mouse model allowed for the delivery of highly focal x-rays in a manner consistent with the volume of intestine that would be irradiated during the delivery of a clinical dose.

This produced highly focal damage to the intestine, which resembled the type of wound associated with clinical radiation therapy treatment. The disruption in barrier function was accompanied by recruitment and activation of immune cells. Here we have shown for the first time that focal irradiation induces significant infiltration of innate and adaptive immune cells localized to the irradiated area. This correlated with a nonsignificant decrease in neutrophils and monocytes in the peripheral blood, which suggests extravasation of these circulating leukocytes into the irradiated intestine 1 day post-IR. This is also consistent with intravital microscopy after 19 Gy, which showed that leukocyte rolling and adhesion in the irradiated intestine began within the first 24 hours post-IR.<sup>21</sup> The irradiated intestine became an inflammatory organ, leading to systemic inflammation and anemia. Anemia is a common complication of cancer that is often further exacerbated by radiation therapy.<sup>22</sup> Understanding the systemic and local effects of radiation therapy has proved important in developing translational therapies.

Intestinal immune cells are likely regulatory both in terms of acute and delayed intestinal radiation injury. In the acute phase, inflammation appears to be necessary to trigger tissue regeneration by targeting both stem cells and differentiated cells.<sup>23</sup> However, in the context of delayed radiation injury, the perpetuation of inflammation appears to be deleterious, as evidenced by eosinophil<sup>24</sup> or macrophage<sup>25</sup> ablation reducing fibrosis. Thus, investigating immune-related cytokines in the context of radiation injury will likely provide mechanistic insight that is relevant both to clinical radiation therapy and to the response to nuclear and radiologic disasters.

IL-6 emerged as an interesting target for study with massive systemic increases in expression in the acute phase post-IR. Surprisingly, histologic examination of IL-6<sup>-/-</sup> mice post-IR found worsened epithelial injury with increased apoptosis and increased baseline cell proliferation compared with IL-6<sup>+/+</sup> mice post-IR, representing an increase in cell turnover. This finding is in agreement with the previously proposed notion that IL-6 and STAT3, the downstream transcription factor activated by IL-6, are necessary for intestinal

epithelial cell survival.<sup>15,16</sup> The analysis of IL-6 blockade in late injury found this was also exacerbated with epithelial erosion and worsened fibrosis in anti-IL-6R-treated mice. This contrasts with mast cell deficient rats,<sup>26</sup> sensory nerve ablated rats,<sup>27</sup> and TGF- $\beta$  heterozygous rats<sup>28</sup> that have exhibited a dichotomous response in the context of acute and late radiation injury, with worsened acute injury and improved late injury. The IL-6 blockade has been demonstrated to ameliorate fibrosis in the lung post-IR.<sup>13</sup> However, this blocked trans signaling rather than the blockade against classical signaling used in this study, which appears to be necessary for the intestinal response to radiation injury. More specific modulation of this signaling pathway may lead to future therapeutic options. Furthermore, our single dose caused an extensive initial injury that developed rapidly compared with what is observed clinically. Therefore, assessment of intestinal injury under various fractionation schemes using this model is also warranted.

## Conclusions

The mucosal ulceration in IL-6<sup>+/+</sup> mice post-IR with consequent bleeding, inflammation, and possible opportunistic infections also led to major systemic effects, including anemia, systemic leukocyte activation, and upregulation of acute phase proteins. This suggests that we are adequately able to model complex multiorgan interactions involved in the pathogenesis of intestinal radiation injury. Furthermore, we were able to reliably cause fibrosis and bowel obstruction, providing suitable endpoints for additional study.

We also demonstrated that IL-6 is important in the intestinal response to focal irradiation both in the acute and late phases using knockout mice and blockade of classical IL-6 signaling. The increased cell turnover observed in IL-6<sup>-/-</sup> mice post-IR suggests IL-6 is necessary for intestinal epithelial cell survival after insult. Furthermore, the worsened epithelial injury and fibrosis in anti-IL-6R treated mice is indicative of a longitudinal importance of IL-6 expression in responding to focal irradiation.

## Supplementary Material

Refer to Web version on PubMed Central for supplementary material.

## Acknowledgments—

The authors thank Khayrullo Shoniyozov for his assistance with the Small Animal Radiation Research Platform. They thank the University of Pennsylvania Veterinary Comparative Pathology Core and Clinical Laboratory for their valuable assistance with this project. They also thank the University of Pennsylvania Diabetes Research Center for the use of the Biomarkers Core (P30-DK19525).

This work was supported by development funds from the Department of Radiation Oncology, Perelman School of Medicine, University of Pennsylvania. B.I.B. and S.K. were supported by the Summer Undergraduate Program for Educating Radiation Scientists Fellowship (R25-CA140116-08).

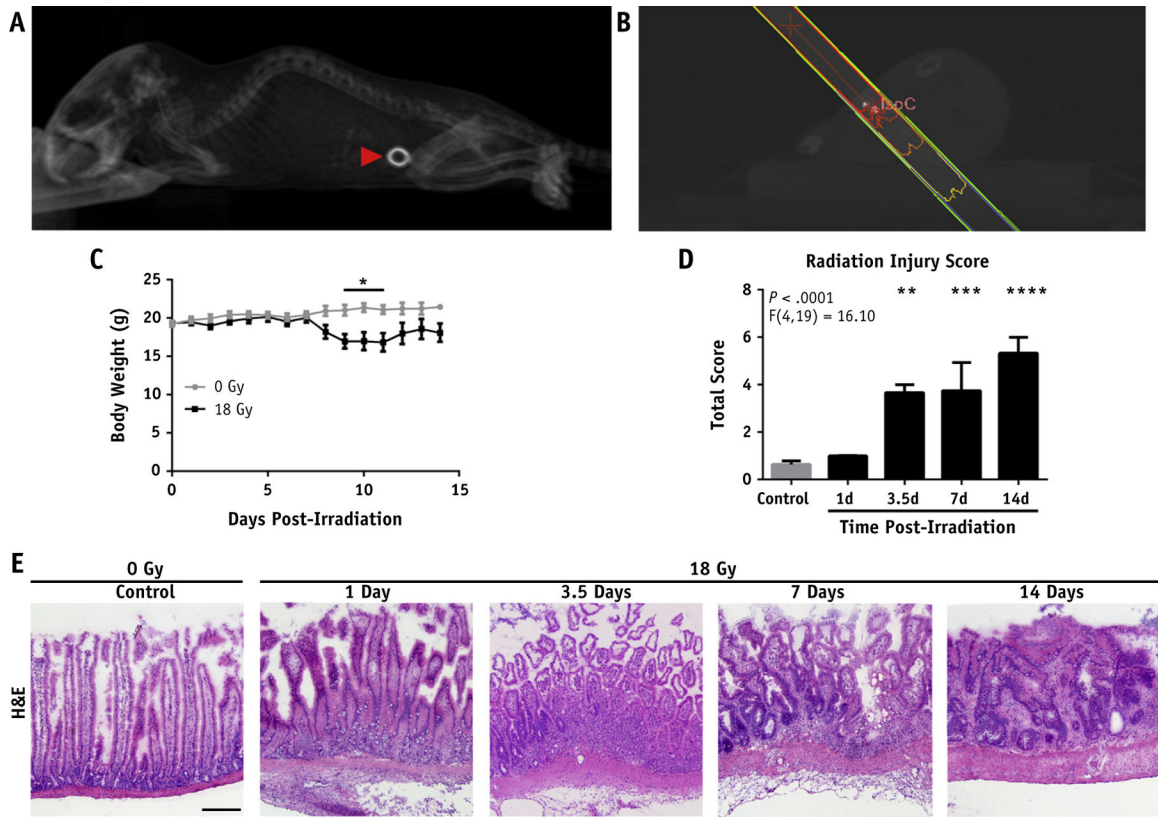
## References

1. Barton MB, Jacob S, Shafiq J, et al. Estimating the demand for radiation therapy from the evidence: A review of changes from 2003 to 2012. *Radiat Ther Oncol* 2014;112:140–144.

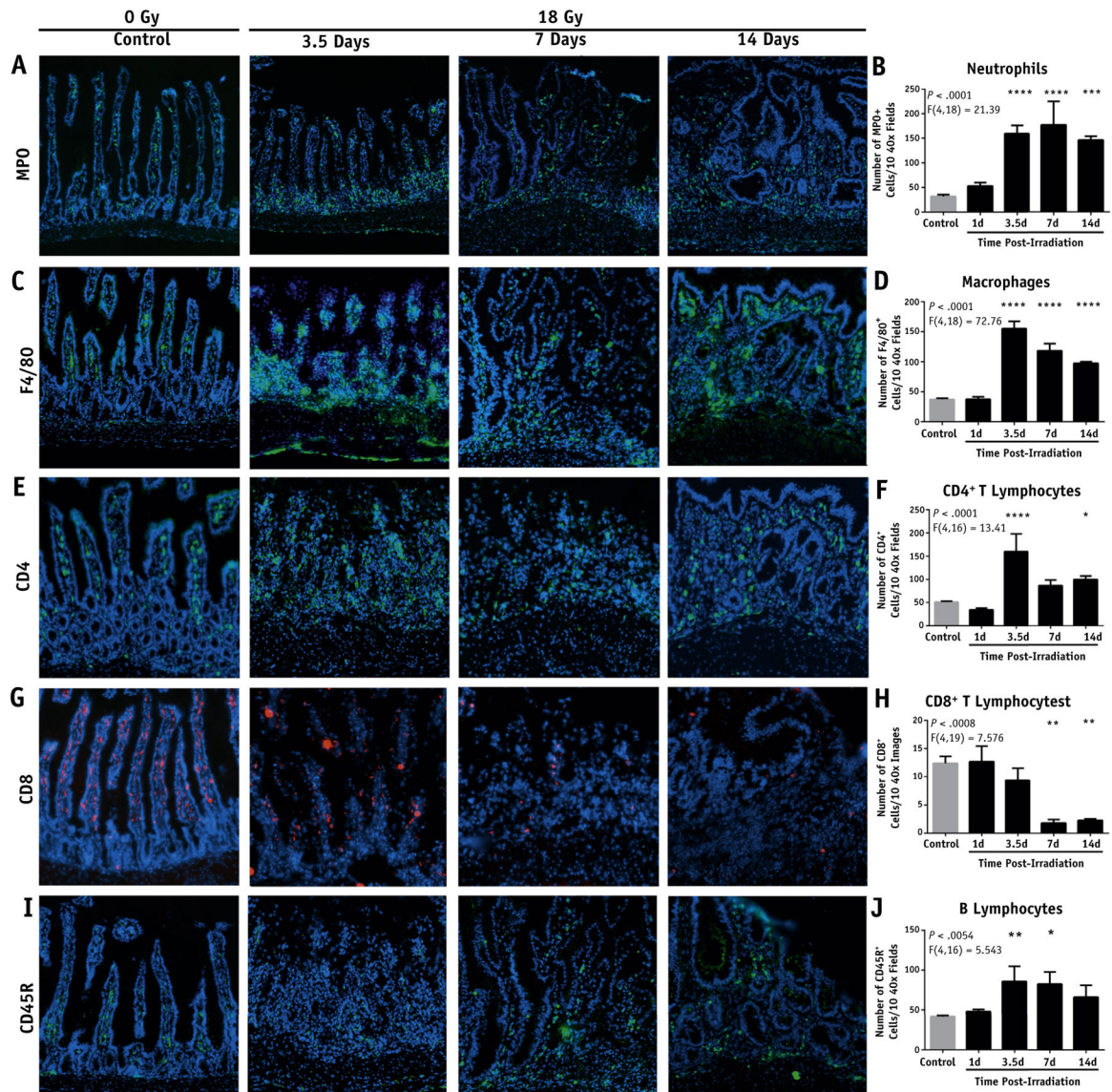


2. Delaney G, Jacob S, Featherstone C, Barton M. The role of radiation therapy in cancer treatment: Estimating optimal utilization from a review of evidence-based clinical guidelines. *Cancer* 2005;104:1129–1137. [PubMed: 16080176]
3. Andreyev HJN. Gastrointestinal problems after pelvic radiation therapy: The past, the present and the future. *Clin Oncol* 2007;19:790–799.
4. Do NL, Nagle D, Poylin VY. Radiation proctitis: Current strategies in management. *Gastroenterol Res Pract* 2011;2011:917941. [PubMed: 22144997]
5. Hauer-Jensen M, Denham JW, Andreyev HJN. Radiation enteropathy–pathogenesis, treatment and prevention. *Nature reviews. Gastroenterol Hepatol* 2014;11:578.
6. Mowat AM, Agace WW. Regional specialization within the intestinal immune system. *Nat Rev Immunol* 2014;14:667–685. [PubMed: 25234148]
7. Grémy O, Benderitter M, Linard C. Acute and persisting Th2-like immune response after fractionated colorectal gamma-irradiation. *World J Gastroenterol* 2008;14:7075–7085. [PubMed: 19084914]
8. Grémy O, Benderitter M, Linard C. Caffeic acid phenethyl ester modifies the Th1/Th2 balance in ileal mucosa after  $\gamma$ -irradiation in the rat by modulating the cytokine pattern. *World J Gastroenterol* 2006; 12:4996–5004. [PubMed: 16937495]
9. Linard C, Marquette C, Mathieu J, et al. Acute induction of inflammatory cytokine expression after  $\gamma$ -irradiation in the rat: Effect of an NF- $\kappa$ B inhibitor. *Int J Radiat Oncol Biol Phys* 2004;58:427–434. [PubMed: 14751512]
10. Richter KK, Langberg CW, Sung C, Hauer-Jensen M. Increased transforming growth factor  $\beta$  (TGF- $\beta$ ) immunoreactivity is independently associated with chronic injury in both consequential and primary radiation enteropathy. *Int J Radiat Oncol Biol Phys* 1997;39:187–195. [PubMed: 9300754]
11. Verginadis II, Kanade R, Bell B, Koduri S, Ben-Josef E, Koumenis C. A Novel Mouse Model to Study Image-Guided, Radiation-Induced Intestinal Injury and Preclinical Screening of Radioprotectors. *Cancer Res* 2017;77:908–917. [PubMed: 28011621]
12. Hunter CA, Jones SA. IL-6 as a keystone cytokine in health and disease. *Nature Immunol* 2015;16:448–457. [PubMed: 25898198]
13. Le TT, Karmouty-Quintana H, Melicoff E, et al. Blockade of IL-6 trans signaling attenuates pulmonary fibrosis. *J Immunol* 2014;193: 3755–3768. [PubMed: 25172494]
14. Fielding C, Jones G, McLoughlin R, et al. Interleukin 6 signaling drives fibrosis in unresolved inflammation. *Immunity* 2014;40:40–50. [PubMed: 24412616]
15. Jin X, Zimmers TA, Zhang Z, et al. Interleukin 6 is an important in vivo inhibitor of intestinal epithelial cell death in mice. *Gut* 2010; 59:186–196. [PubMed: 19074180]
16. Grivennikov S, Karin E, Terzic J, et al. IL-6 and Stat3 are required for survival of intestinal epithelial cells and development of colitis-associated cancer. *Cancer Cell* 2009;15:103–113. [PubMed: 19185845]
17. Langberg CW, Sauer T, Reitan JB, Hauer-Jensen M. Relationship between intestinal fibrosis and histopathologic and morphometric changes in consequential and late radiation enteropathy. *Acta Oncologica* 1996;35:81–87.
18. Bhatia M, Moochhala S. Role of inflammatory mediators in the pathophysiology of acute respiratory distress syndrome. *J Pathol* 2004;202:145–156. [PubMed: 14743496]
19. Hartman MHT, Vreeswijk-Baudoin I, Groot HE, et al. Inhibition of interleukin 6 receptor in a murine model of myocardial ischemia-reperfusion. *PLoS One* 2016;11:e0167195. [PubMed: 27936014]
20. Lattouf R, Younes R, Lutomski D, et al. Picosirius red staining: A useful tool to appraise collagen networks in normal and pathologic tissues. *J Histochem Cytochem* 2014;62:751–758. [PubMed: 25023614]
21. Johnson LB, Riaz AA, Adawi D, et al. Radiation enteropathy and leukocyte-endothelial cell reactions in a refined small bowel model. *BMC Surg* 2004;4:10. [PubMed: 15363103]
22. Harrison L, Shasha D, Shiaoova L, et al. Prevalence of anemia in cancer patients undergoing radiation therapy. *Semin Oncol* 2001;28:54–59.

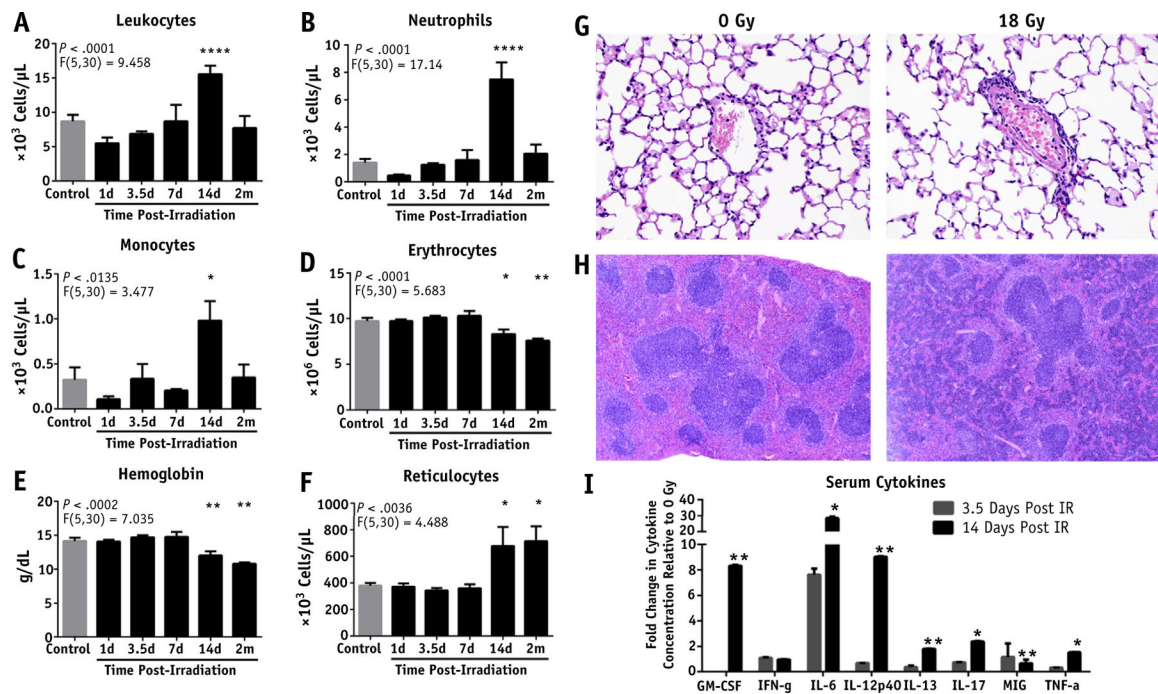
23. Karin M, Clevers H. Reparative inflammation takes charge of tissue regeneration. *Nature* 2016;529:307–315. [PubMed: 26791721]
24. Takemura N, Kurashima Y, Mori Y, et al. Eosinophil depletion suppresses radiation-induced small intestinal fibrosis. *Sci Transl Med* 2018;10:429.
25. Loinard C, Vilar J, Milliat F, et al. Monocytes/macrophages mobilization orchestrate neovascularization after localized colorectal irradiation. *Radiat Res* 2017;187:549–561. [PubMed: 28319461]
26. Zheng H, Wang J, Hauer-Jensen M. Role of mast cells in early and delayed radiation injury in rat intestine. *Radiat Res* 2000;153:533–539. [PubMed: 10790274]
27. Wang J, Zheng H, Kulkarni A, et al. Regulation of early and delayed radiation responses in rat small intestine by capsaicin-sensitive nerves. *Int J Radiat Oncol Biol Phys* 2006;64:1528–1536. [PubMed: 16580503]
28. Wang J, Zheng H, Hauer-Jensen M. Influence of short-term octreotide administration on chronic tissue injury, transforming growth factor  $\beta$  (TGF- $\beta$ ) overexpression, and collagen accumulation in irradiated rat intestine. *J Pharmacol Exp Ther* 2001;297:35–42. [PubMed: 11259525]



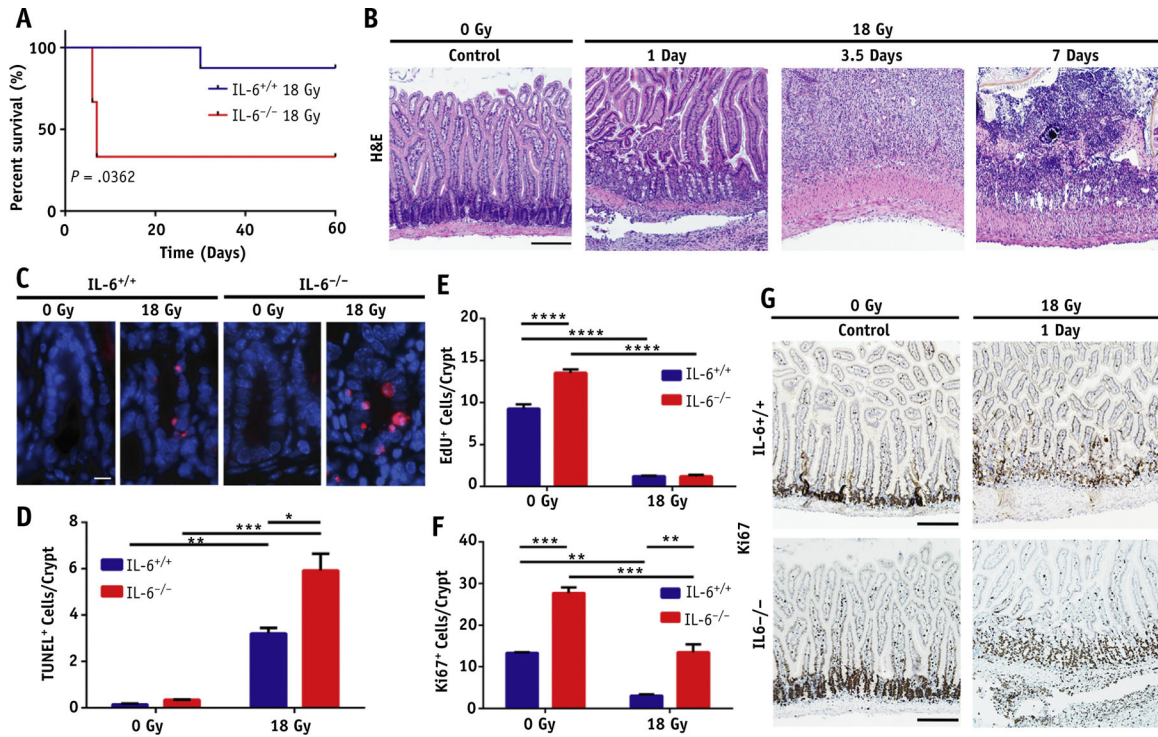
**Fig. 1.** Focal irradiation (IR) produces localized damage. (A) Three-dimensional rendering of a sagittal view of a cone beam computed tomography (CT) scan showing implanted marker (red arrowhead). (B) Dose plan in MuriPlan. (C) Body weights post-IR. (D) Radiation injury scoring of the marked intestine at the indicated times post-IR. (E) Representative hematoxylin and eosin (H&E) stained frozen sections of the marked intestine post-IR (10× magnification; scale bar, 50 μm).  $P < .05$  (\*),  $P < .01$  (\*\*),  $P < .001$  (\*\*\*),  $P < .0001$  (\*\*\*\*).



**Fig. 2.** Evaluation of leukocyte infiltration into the intestine after focal irradiation (IR). Representative images of the marked intestine after a single dose of 18 Gy and the quantification of positive stained cells per 10 40× fields. (A, B) Myeloperoxidase<sup>+</sup> cells. (C, D) F4/80<sup>+</sup> cells. (E, F) CD4<sup>+</sup> T cells. (G, H) CD8<sup>+</sup> T cells. (I, J) CD45R<sup>+</sup> B cells (stitched 40× magnification; scale bar, 50 μm).  $P < .05$  (\*),  $P < .01$  (\*\*),  $P < .001$  (\*\*\*),  $P < .0001$  (\*\*\*\*).

**Fig. 3.**

Systemic inflammatory response and anemia induced by focal irradiation (IR) of the intestine. Effect of focal, single dose 18 Gy on (A) leukocytes, (B) neutrophils, (C) monocytes, (D) erythrocytes, (E) hemoglobin, and (F) reticulocytes in the peripheral blood as assessed by complete blood count. (G) Hematoxylin and eosin (H&E) stained sections of the lung 2 weeks post-IR (40 $\times$  magnification; scale bar, 50  $\mu$ m). (H) H&E stained sections of the spleen 2 weeks post-IR (diffuse basophilic staining in red pulp; 10 $\times$  magnification; scale bar, 200  $\mu$ m). (I) Multiplex cytokine microbead assay on serum cytokines at 3.5 and 14 days post-IR, normalized to 0 Gy controls.  $P < .05$  (\*),  $P < .01$  (\*\*),  $P < .0001$  (\*\*\*\*).

**Fig. 4.**

Interleukin 6 (IL-6) knockout mice are sensitized to intestinal irradiation (IR) in the acute phase. (A) Survival proportions of IL-6<sup>+/+</sup> and IL-6<sup>-/-</sup> mice after 18 Gy of focal IR. (B) Hematoxylin and eosin (H&E) staining of the marked intestinal segments in IL-6<sup>-/-</sup> mice post-IR (10× magnification; scale bar, 50 μm). (C) Representative images of TUNEL<sup>+</sup> cells/crypt in IL-6<sup>+/+</sup> and IL-6<sup>-/-</sup> mice 24 hours post-IR (63× magnification; scale bar, 10 μm). (D) Quantification of TUNEL<sup>+</sup> cells/crypt. (E) Quantification of EdU<sup>+</sup> cells/crypt. (F) Quantification of Ki67<sup>+</sup> cells/crypt. (G) Representative images of Ki67 staining in the intestines of IL-6<sup>+/+</sup> and IL-6<sup>-/-</sup> mice 24 hours post-IR (10× magnification; scale bar, 50 μm). *P* < .05 (\*), *P* < .01 (\*\*), *P* < .001 (\*\*\*), *P* < .0001 (\*\*\*\*).

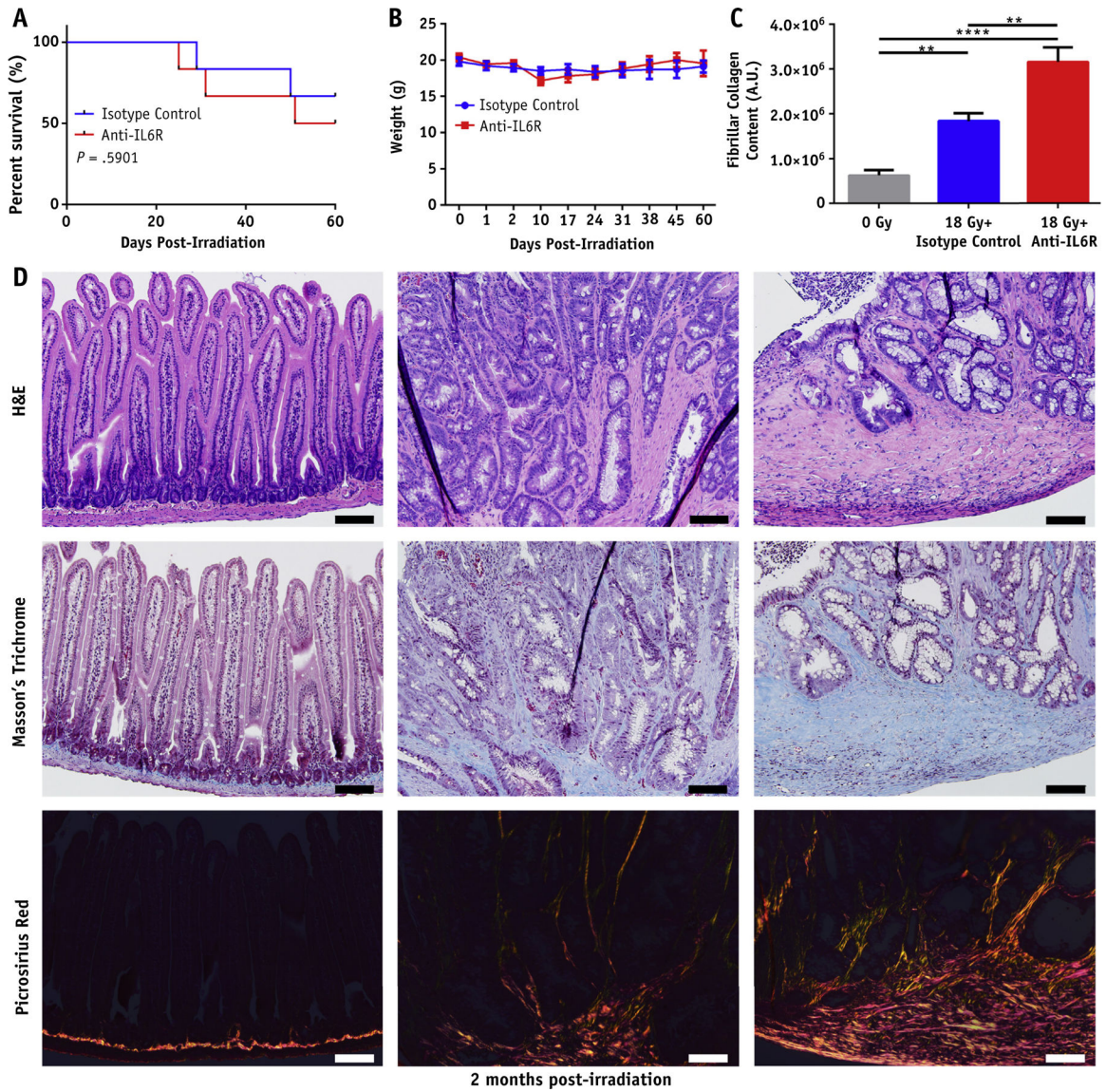


**Fig. 5.** Antibody mediated blockade of interleukin 6 (IL-6) signaling exacerbates intestinal fibrosis post-irradiation (IR). (A) Kaplan-Meier survival analysis of isotype and anti-IL-6R-treated mice after 18 Gy. (B) Body weights of isotype and anti-IL-6R-treated mice post 18 Gy. (C) Quantification of fibrillar collagen content performed in ImageJ. (D) Hematoxylin and eosin (H&E), Masson's trichrome, and picrosirius red stained sections of intestine from control, 18 Gy + isotype treated mice, and 18 Gy + anti-IL-6R-treated mice 2 months post-IR (20 magnification, scale bar 100 μm).  $P < .01$  (\*\*),  $P < .0001$  (\*\*\*\*).